



Effects of thiourea on the kinetics and electrochemical nucleation of tin electrodeposition from stannous chloride bath in acidic medium

FATIMA KESRI, ABED M. AFFOUNE* and ILHEM DJAGHOUT

Laboratoire d'Analyses Industrielles et Génie des Matériaux, Département de Génie des Procédés, Faculté des Sciences et de la Technologie, Université 8 Mai 1945 Guelma, BP 401, Guelma 24000, Algeria

(Received 25 March, revised 18 November, accepted 10 December 2018)

Abstract: The effects of thiourea (TU) on the kinetics and electrochemical nucleation of tin from stannous chloride bath in acidic medium have been investigated by cyclic voltammetry (CV), electrochemical impedance spectroscopy (EIS) and chronoamperometry. CV results showed that the tin reduction is a one-step reaction and indicated that TU inhibited the reduction of tin ions at high concentration. EIS analysis showed that the electrodeposition process of tin is affected by the addition of TU. The nucleation mechanism of tin was studied using both Sharifker–Hills (SH) and Palomar–Pardavé (PP) models. SH model indicated that hydrogen evolution and tin reduction occurred simultaneously. Non-dimensional current-time transients curves based on PP model revealed that the tin nucleation followed 3D progressive mechanism without TU and with 0.01 M TU, while the nucleation process changes to 3D instantaneous in presence of 0.1 M TU. However, at 1 M TU, the nucleation mechanism is located between instantaneous and progressive model. The proton reduction reaction was inhibited at all concentrations of TU. Quantitative determination showed that in the presence of TU, the diffusion coefficient of tin species, the hydrogen evolution rate constant, the nucleation rate constant and the number of active sites were decreased.

Keywords: tin chloride; additives; cyclic voltammetry; chronoamperometry; Sharifker–Hills model; Palomar–Pardavé model.

INTRODUCTION

Tin and its alloys play a very important role in surface treatments, electrical, electronic and microelectronic technologies, because of their specific characteristics such as: non-toxicity, ductility, malleability, and high corrosion resistance.¹ Furthermore, tin and its alloys have been used as: anodic materials in lithium and sodium-

*Corresponding author. E-mail: affoune2@yahoo.fr
<https://doi.org/10.2298/JSC180325107K>

-ion batteries,²⁻⁵ semiconductor materials in solar cells,⁶ photocatalysts for photo-degradation of organic compounds⁷ and as a catalyst for methanol oxidation in fuel cells.⁸

Electrodeposition of tin and its alloys is generally carried out using sulphate or chloride based stannous baths, in acidic⁹⁻²¹ or alkaline^{22,23} media. In literature, other types of baths such as: fluoroborates,²⁴ pyrophosphates^{2,25} and methanosulfonates^{26,27} have been also reported.

Recently, acidic stannous baths are mainly used for tin electrodeposition because they operate at ambient temperature and increase the deposition rate. Tin electrodeposits in the absence of additives are porous, non-adherent, non-bright and whiskery. Hence, organic additives must be added to the baths in order to stabilize tin ions which allows the control of the deposition kinetics and improves the morphological and structure properties. These additives can play the role of antioxidant agents,¹⁷ brighteners,¹⁴⁻¹⁶ grain refiners,^{14,15} complexing agents^{11,12,14,29} and surfactants.^{15,18,30} Thiourea (TU) is among additives which are frequently used in tin baths. The effect of TU on the morphology and microstructure of tin and tin alloys have been studied.^{15,28} Only very few reports discussed the effect of TU on the tin nucleation from a sulphate bath.³¹ However, and as far as we know, no investigation has been made on the nucleation mechanism of tin from chloride baths in the presence of TU.

In this work we study the role of thiourea on the kinetics, electrochemical nucleation and hydrogen evolution during the electrodeposition of tin from acidic chloride baths.

EXPERIMENTAL

The main electrolytic bath was prepared by dissolving tin chloride ($\text{SnCl}_2 \cdot 2\text{H}_2\text{O}$) in distilled water followed by a gradual addition of sulfuric acid (H_2SO_4). The pH of the mixture is 0.3. Different baths are prepared by addition of thiourea ($\text{CH}_4\text{N}_2\text{S}$) at different concentrations to the main bath (Table I).

TABLE I. Chemical composition of plating baths (mol dm⁻³)

No.	$\text{SnCl}_2 \cdot 2\text{H}_2\text{O}$	H_2SO_4	$\text{CH}_4\text{N}_2\text{S}$
1	0.14	2.0	—
2	0.14	2.0	0.01
3	0.14	2.0	0.1
4	0.14	2.0	1.0

The electrochemical experiments have been performed in a three-electrode cell at room temperature. The working electrode was a copper sheet with an area of 1.57 cm². A platinum wire was used as counter electrode, and a saturated calomel electrode (SCE) as reference electrode. All the potentials were expressed with respect to the reference electrode. Before each experiment, the working electrode was polished by abrasive paper of 800, 1200 and 2000 grits. Then, it was thoroughly degreased with detergent and rinsed using tap water. After being dried, the copper substrates were degreased with sodium hydroxide at 50 °C during 5

min and then immediately immersed in concentrated sulphuric acid to remove any surface oxides³². Finally, the substrates were rinsed with distilled water and then dried.

Cyclic voltammetry (CV) and chronoamperometry (CHR) experiments were carried out using an EG & G Princeton Applied Research potentiostat/galvanostat, model 273A, controlled by Power Suite software. The Electrochemical impedance spectroscopy (EIS) measurements have been performed using Gamry potentiostat/galvanostat/ZRA, model Interface 1000. The impedance spectra were measured at -0.6 V with the sinusoidal perturbation of 5 mV from 10 kHz to 10 mHz. X-ray diffraction analysis of tin electrodeposits was conducted using a Bruker D8 Advance X-ray diffractometer (CuK radiation). The complexation phenomena of tin species were analysed by UV–Vis absorption spectrophotometer (Jenway, 7135) in a wavelength range between 200 and 800 nm.

RESULTS AND DISCUSSION

Kinetics study

Typical voltammograms of tin ions reduction in the absence and the presence of TU are presented in Fig. 1. In this figure, we observe a cathodic peak during the forward scan followed by an anodic peak during the return scan. The rapid fall of the current after anodic peak indicated the dissolution of metallic compounds. It corresponds to the metallic tin formed during the cathodic polarization according to the following reaction:

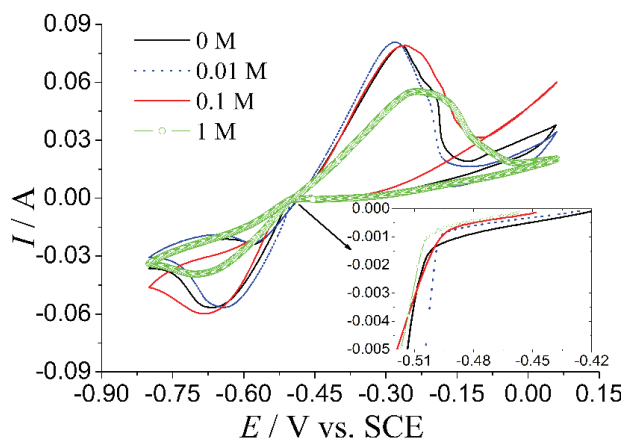


Fig. 1. Cyclic voltammograms of tin baths without and with different concentration of TU at scan rate 100 mV s⁻¹. The inset shows the open circuit potential (OCP) change as function of TU concentration.

The small shoulder following the anodic peak at -0.2 V can be attributed to the oxidation of Sn to Sn^{4+} .³³ The anodic peak current observed at -0.1 V corresponds to the oxidation of copper substrate. Moreover, the hysteresis recorded during the return scan of voltammograms (Fig. 1) is a characteristic of a three-

-dimensional (3D) nucleation process. The XRD spectra (Fig. 2) confirm that the deposits were mainly consisted of tin metal with the presence of Cu₆Sn₅ phase.

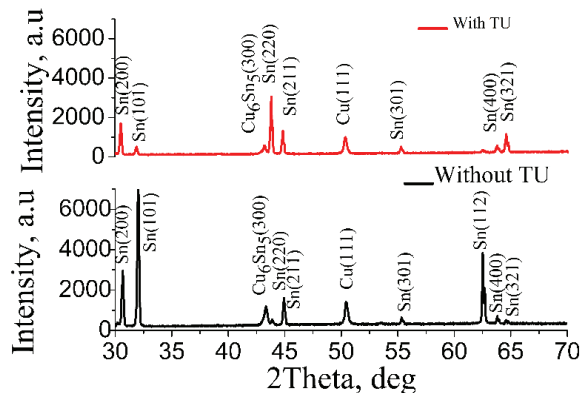


Fig. 2. X-ray diffraction pattern of tin electrodeposited without TU and with 1.0 M TU.

The voltammetric curves show that the addition of TU decreases the current values of cathodic peaks at high concentrations. This indicated an inhibition effect of additives which could be attributed to their adsorption at active sites on the electrode surface. The inset of Fig. 1 shows the evolution of the open circuit potential as a function of the addition of TU. It appears that TU has a slightly significant influence on this potential. This feature is the characteristic of the possible complexation reaction between tin ions and TU. The absorbance of tin ions solution in the presence of 0.01 M TU solution were recorded using UV–Vis spectrophotometry (Fig. 3).

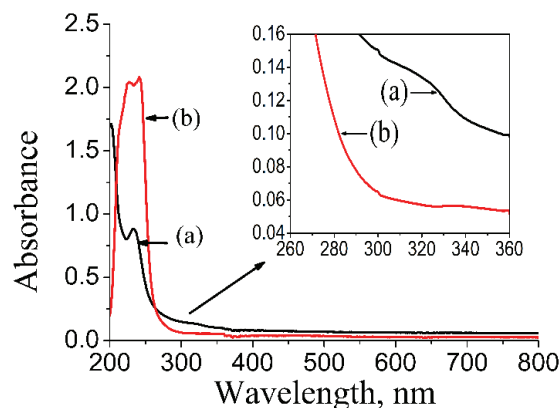


Fig. 3. UV–Vis absorbance spectra of baths: a) without TU and b) with 0.01 M TU. Inset shows the magnified spectra in the range between 260 and 360 nm.

The spectra show the appearance of one peak at 233 nm followed by a shoulder between 300 and 340 nm in absence of TU. These could be ascribed to the presence of [Sn(H₂O)₆]²⁺ and [Sn(SO₄)₂]²⁻, respectively. The addition of TU

shows two absorption bands at 226 and 239 nm, which could be assigned to $\pi-\pi^*$ transition in TU molecule.³⁴ A further insight reveals a decrease in the shoulder absorbance with TU (as shown in the inset of Fig. 3). This indicates a possible interaction between tin ions and TU molecules.³⁵ Hence, the formation of tin complexes might be responsible for the shift of OCP to cathodic values.

In order to understand better the kinetics of the tin reduction process with and without TU, the electrochemical impedance spectroscopy has been used to characterize the electrode-electrolyte interface. Nyquist plots (Fig. 4) show two capacitive loops in the high and low frequency ranges with and without TU. The first semicircle at high frequency (HF) could be associated with the solid electrolyte interface film (SEI), while the second semicircle at low frequency (LF) is assigned to the charge transfer resistance (R_{ct}). The addition of TU causes a decrease in capacitive loops at the low frequency. The similar results are reported by others authors.^{28,31,39} The equivalent circuit which fitted the experimental data is depicted in Fig. 5. This circuit is described by two constant phase elements in series. It consists of a solution resistance R_1 , SEI resistance R_2 , constant phase elements (CPE) Q_2 associated to SEI, charge transfer resistance R_3 and constant phase elements (CPE) Q_3 associated to double layer interface.

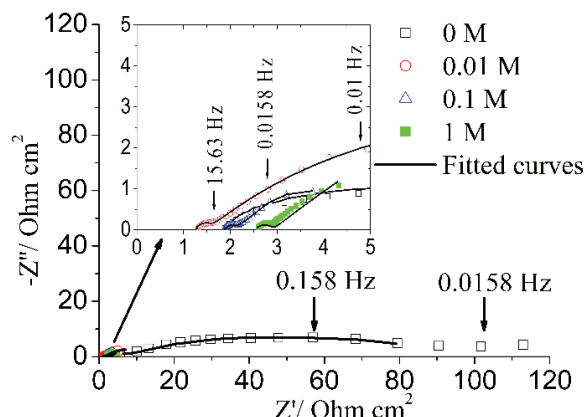


Fig. 4. Nyquist plots obtained at -0.6 V for tin electrodeposition without and with TU.

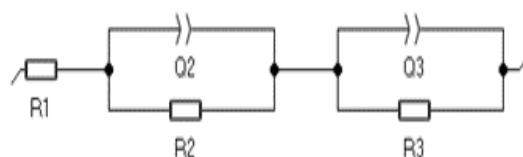


Fig. 5. Equivalent circuit used to fit the experimental impedance data.

The impedance of a constant phase element (CPE) is defined as:

$$Z_{\text{CPE}} = \frac{1}{Q(i\omega)^\alpha} \quad (2)$$

where $i^2 = -1$ and $\omega = 2\pi f$ is the angular frequency. The dimensionless exponent α characterizes the nature of CPE.

The obtained results are presented in Table II. The R_{ct} values of Table II represent R_3 values of fitting results reported in Table S-I of the Supplementary material to this paper. The decreases in R_{ct} values after addition of TU indicates that the charge transfer rate involving tin thiourea complex ions is higher than that of hydrated tin ions. These results could be explained by the presence of sulphur atoms in TU molecules structure, which facilitates the electrons transfer between electrode surface and stannous ions, when adsorbed on copper substrate.³⁵ The comparison between the cathodic peak current density values i_{pc} (Table II) shows that the lower value of i_{pc} is obtained at 1.0 M, which indicated that the inhibition effect of TU at this concentration is predominant. This inhibition is probably due to the adsorption of TU molecules on active sites of electrode area.

TABLE II. Charge transfer resistance R_{ct} , and cathodic peak current-density i_{pc} as function of TU concentrations

TU concentration, M	$R_{\text{ct}} / \Omega \text{ cm}^2$	$i_{\text{pc}} / \text{A cm}^{-2}$
0	83.04	0.035
0.01	7.85	0.036
0.1	4.63	0.038
1	6.25	0.025

Nucleation and hydrogen evolution study

The tin nucleation process on copper electrode was analyzed by recording the chronoamperometric curves at different potentials without and with TU (Figs. 6 and 7).

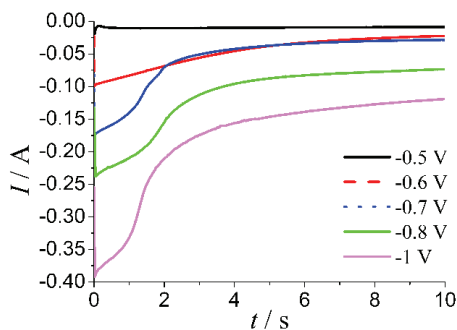


Fig. 6. Chronoamperogramms for tin electro-deposition without TU at different potentials.

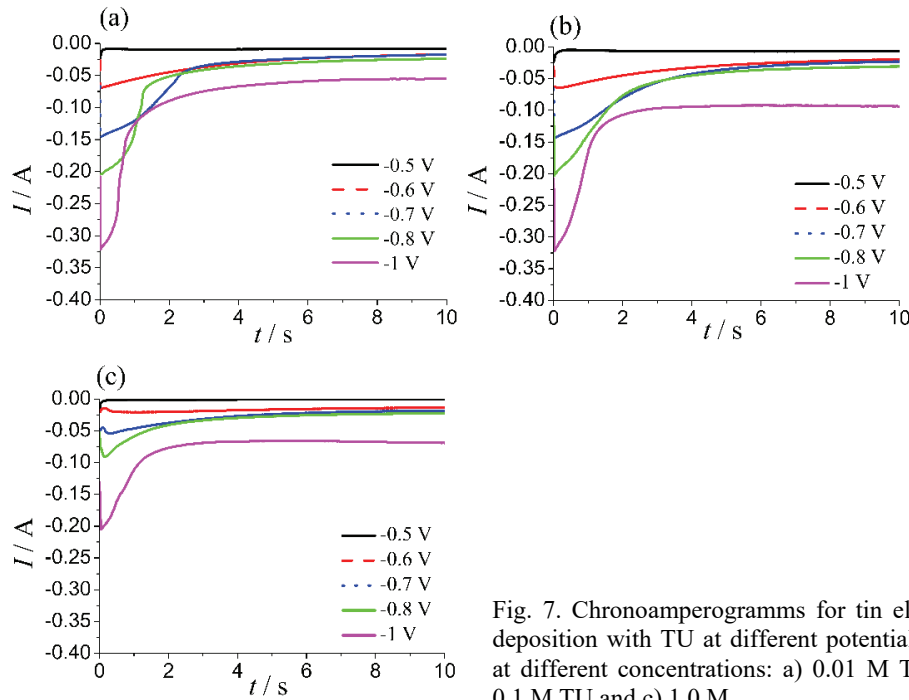


Fig. 7. Chronoamperogramms for tin electrodeposition with TU at different potentials and at different concentrations: a) 0.01 M TU, b) 0.1 M TU and c) 1.0 M.

The chronoamperograms presented a relatively similar behaviour and they are characterized by an increase in the current at first instants, up to a maximum value (I_{\max}) at a deposition time (t_{\max}). The maximum value of the current is due to the formation and growth of the tin germs. It is followed by a gradual decrease in the current imposed by the diffusion of the ions towards the electrode surface.

To identify nucleation–growth mechanisms, non-dimensional curves of the form $I / I_{\max} = f(t / t_{\max})$ have been built from the experimental chronoamperograms of Figs. 6 and 7. These curves were compared with the theoretical curves of Scharifker–Hills³⁶ related to the instantaneous and progressive nucleation mechanisms, followed by the three-dimensional diffusion-limited growth. The mathematical relationships of the instantaneous and progressive nucleation in the case of 3D growth are respectively given by the following equations:

$$\frac{I^2}{I_{\max}^2} = 1.9542 \left(\frac{t_{\max}}{t} \right) \left[1 - \exp \left(-1.2564 \frac{t}{t_{\max}} \right) \right]^2 \quad (3)$$

$$\frac{I^2}{I_{\max}^2} = 1.2254 \left(\frac{t_{\max}}{t} \right) \left[1 - \exp \left(-2.3367 \frac{t^2}{t_{\max}^2} \right) \right]^2 \quad (4)$$

Comparison between the experimental and the theoretical curves of the instantaneous and progressive 3D nucleation models in different concentrations of TU at different potentials are presented in Figs. 8 and 9.

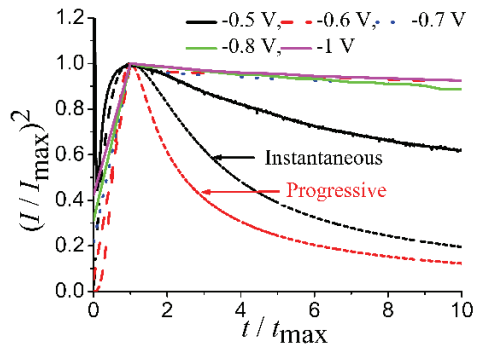


Fig. 8. Comparison between non-dimensional experimental and theoretical curves of 3D instantaneous and progressive nucleation models for tin electrodeposition without TU at different potentials.

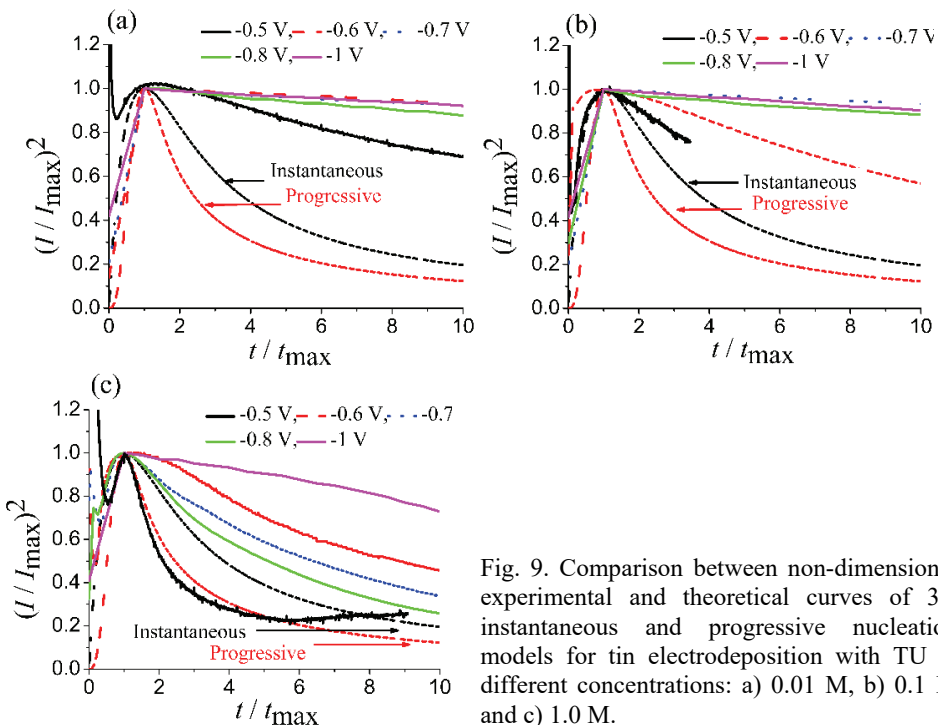


Fig. 9. Comparison between non-dimensional experimental and theoretical curves of 3D instantaneous and progressive nucleation models for tin electrodeposition with TU at different concentrations: a) 0.01 M, b) 0.1 M and c) 1.0 M.

We observe that calculated curves present a deviation beyond the maximum peak of the dimensionless current, which is generally attributed to the hydrogen evolution.³⁷ Hence it is difficult to pronounce whether the nucleation mechanism of tin is progressive or instantaneous, using the Sharifker–Hills model. In order to separate the contribution of hydrogen reaction from the total current, we used the

Palomar–Pardavé model.³⁷ This latter assumes that the total cathodic current consists of two terms: the first is the proton reduction and the second is the tin reduction according to the following equation:

$$i_t = \left(P_1^* + P_4 t^{-0.5} \right) \left(1 - \exp \left(-P_2 \left[t - \frac{1 - \exp(-P_3 t)}{P_3} \right] \right) \right) \quad (5)$$

The unknown parameters in the Eq. (5) are defined as:

$$P_1^* = zFk_{\text{PR}} \left(\frac{2Mc}{\pi\rho} \right)^{0.5} \quad (6)$$

$$P_2 = D\pi N_0 \left(\frac{8\pi c}{\rho} \right)^{0.5} \quad (7)$$

$$P_3 = A \quad (8)$$

$$P_4 = 2Fc \left(\frac{D}{\pi} \right)^{0.5} \quad (9)$$

where c is the concentration of metal ions, M is the molar mass of deposit, ρ is the density of deposit, N_0 is the number of active site, D is the diffusion coefficient of metal ion, A is the nucleation rate constant, k_{PR} is rate constant of proton reduction and z is the number of electrons transferred during the hydrogen ions reaction. The constants P_1^* , P_2 , P_3 and P_4 could be determined from fitting the experimental current transients using the non-linear Levenberg–Marquardt algorithm method.

The best fitting of experimental data (Fig. 10a) using Palomar–Pardavé model is obtained at –0.6 V (Fig 10c). Palomar fittings indicated that the current of tin reduction decreases in the presence of TU (Fig. 10c). Sharifker–Hills model applied on the curves of tin (Fig. 10a and c) is presented in Fig. 10b and d, respectively. Results show clearly that the nucleation of tin mechanism is almost progressive without TU and with 0.01 M TU and that the addition of TU at higher concentration change the nucleation mechanism. At 0.1 M TU, the nucleation process changes to instantaneous nucleation, while at 1 M TU, the nucleation behaviour of tin is located between instantaneous and progressive mechanisms. These results are in agreement with literature.^{31,39} The nucleation mechanism of tin was 3D progressive in the chloride solution,^{11,20,22} while in the sulphate solution instantaneous nucleation mode^{1,16,19} was observed.

The kinetics parameters deduced from the curves presented in Fig. 10c were obtained using Eqs. (6)–(9) and summarized in Table III. The results indicate that there is no significant decrease in the nucleation rate constant A while at 0.01 M and 0.1 M TU concentrations, hydrogen rate constant k_{PR} was significantly reduced.

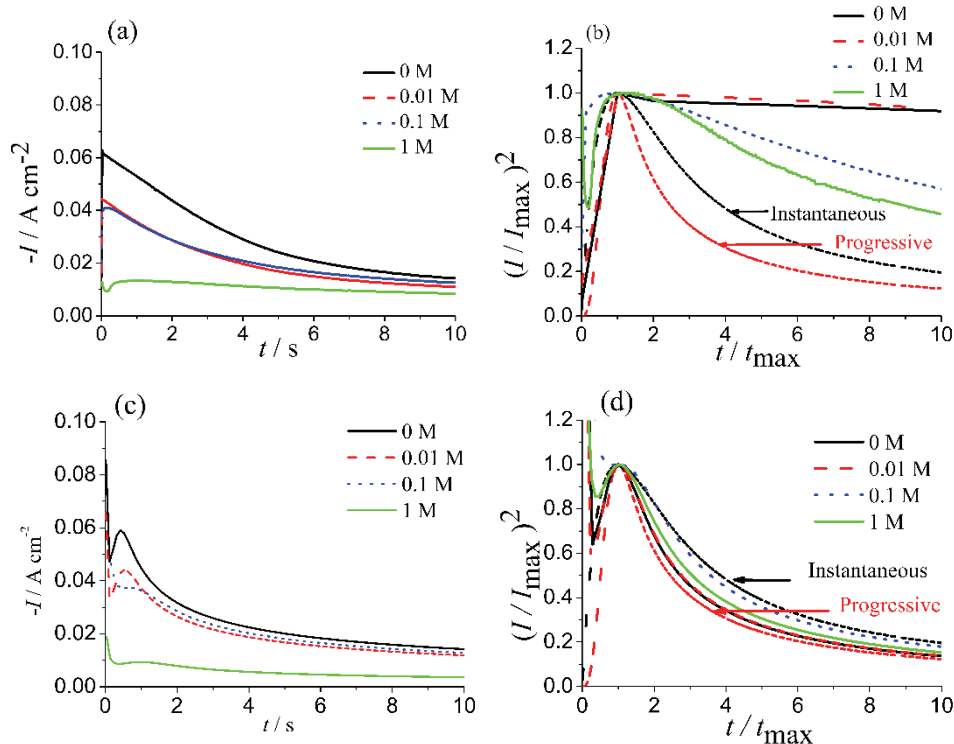


Fig. 10. Current–time transients and their non dimensional curves without and with TU at -0.6 V: a) experimental current–time transients, b) non-dimensional experimental curves of current–time transients presented in (a) compared to theoretical ones of 3D instantaneous and 3D progressive nucleation, c) fitted current–time transients corresponding to tin ions reduction after non-linear fitting of Eq. (5) and d) non-dimensional fitted curves of current–time transients presented in c) compared to theoretical ones of 3D instantaneous and 3D progressive nucleation.

TABLE III. Kinetics parameters resulting from fitting results obtained without and with TU at -0.6V

TU concentration, M	0	0.01	0.1	1
$P_1 \times 10^3 / \text{A cm}^{-2}$	5.56	0.03	0.05	3.36
P_2 / s^{-1}	21.06	14.15	5.05	1.34
$P_3 \times 10 // \text{s}^{-1}$	9.85	9.80	8.99	5.99
$P_4 \times 10^2 / \text{s}^{-1}$	4.49	3.76	4.05	1.61
$A \times 10 / \text{s}^{-1}$	9.85	9.80	8.99	5.99
$D \times 10^6 / \text{cm}^2 \text{s}^{-1}$	8.67	6.05	7.05	1.11
$N_0 \times 10^6 / \text{cm}^{-2}$	3.52	3.39	1.03	1.74
$k_{\text{PR}} \times 10^7 / \text{mol cm}^{-2} \text{s}^{-1}$	7.56	0.04	0.07	4.57

The number of active sites N_0 decreases upon the addition of TU. This is consistent with the adsorption of TU molecules. A similar result has been reported in

the literature by Lie *et al.*,³⁸ which investigated the tin electrodeposition in the presence of amine non-ionic surfactant. We observed that the diffusion coefficient D of tin ions decreases with addition of TU. This indicates that the tin ions complexation by TU leads to relatively heavy tin ions. These values of D are in good agreement with those reported in the literature.^{9,11,20}

CONCLUSION

The effects of TU on the kinetics and electrochemical nucleation of tin from stannous chloride bath in acidic medium were investigated using cyclic voltammetry, electrochemical impedance spectroscopy and chronoamperometry techniques. The cyclic voltammetry measurements showed that TU inhibited the reduction reaction of tin ions at higher concentration. The EIS analysis showed two semicircles in the presence of TU, which indicated that the electrodeposition process of tin was accompanied by the adsorption of electroactive species and tin thiourea complex ions. Sharifker–Hills and Palomar–Pardavé models applied for tin chronoamperogramms revealed that the tin nucleation followed 3D progressive mechanism with and without 0.01 M TU, and the addition of 0.1 and 1.0 M TU changed the nucleation mechanism. The proton reduction reaction was inhibited at all concentrations of TU. The addition of TU decreased the diffusion coefficient D of tin species, as well as the hydrogen rate constant (k_{PR}), the nucleation rate constant (A) and the number of active sites N_0 .

И З В О Д

ЕФЕКАТ ТИОУРЕЕ НА КИНЕТИКУ И ЕЛЕКТРОХЕМИЈСКУ НУКЛЕАЦИЈУ ПРИ
ТАЛОЖЕЊУ КАЛАЈА ИЗ КИСЕЛОГ РАСТВОРА КАЛАЈ(II)-ХЛОРИДА

FATIMA KESRI, ABED M. AFFOUNE и ILHEM DJAGHOUT

Laboratoire d'Analyses Industrielles et Génie des Matériaux, Département de Génie des Procédés, Faculté des Sciences et de la Technologie, Université 8 Mai 1945 Guelma, BP 401, Guelma 24000, Algeria

Ефекат тиоуреје (TU) на кинетику и електрохемијску нуклеацију при таложењу калаја из киселог раствора калај(II)-хлорида испитан је методама цикличне волтаметрије, спектропотенциометрије електрохемијске импеданције и хроноамперометрије. Према резултатима цикличне волтаметрије, редукција калаја се одиграва у једном ступњу, што указује да TU инхибира редукцију јона калаја при високим концентрацијама. Анализа електрохемијске импеданције је такође показала утицај додатка TU на процес таложења калаја. Механизам таложења калаја је анализиран коришћењем модела Sharifker–Hills (SH) и модела Palomar–Pardavé (PP). Модел SH је указао да се издавање водоника и редукција калаја одигравају истовремено. Зависности струје од времена према моделу PP, приказане преко бездимензионих параметара, показале су да нуклеација калаја следи прогресивни 3D механизам без TU и у присуству 0,01 M TU, а прелази у механизам тренутног 3D таложења у присуству 0,1 M TU. Међутим, у раствору који је садржао 1,0 M TU, механизам нуклеације је између тренутног и прогресивног модела. Редукција протона је инхибирана у присуству TU без обзира на њену концентрацију. Квантитативна одређивања су показала да коефицијент дифузије јона калаја, константа брзине издавања водоника, константа брзине нуклеације калаја и број активних места опадају у присуству TU.

(Примљено 25. марта, ревидирано 18. новембра, прихваћено 10. децембра 2018)

REFERENCES

1. F. C. Walsh, C. T. J. Low, *Surf. Coat. Technol.* **288** (2016) (<http://dx.doi.org/10.1016/j.surfcoat.2015.12.081>)
2. R. H. Kim, D. H. Nam, H. S. Kwon, *J. Power Sources* **195** (2010) 506 (<http://dx.doi.org/10.1016/j.jpowsour.2010.01.069>)
3. Z. Du, S. Zhang, T. Jiang, Z. Bai, *Electrochim. Acta* **55** (2010) 3537 (<http://dx.doi.org/10.1016/j.electacta.2010.01.065>)
4. T. Noriyuki, O. Ryuji, F. Masahisa, F. Shin, K. Maruo, Y. Ikuo, *J. Power Sources* **107** (2002) 48
5. L. Luo, H. Qiao, W. Xu, D. Li, J. Zhu, C. Chen, Y. Lu, P. Zhu, X. Zhang, Q. Wei, *J. Solid State-Electrochem.* **21** (2017) 1385 (<http://dx.doi.org/10.1007/s10008-016-3501-3>)
6. S. S. Hortikar, V.S. Kadam, A. B. Rathi, C.V. Jagtap, H. M. Pathan, I. S. Mulla, P.V. Adhyapak, *J. Solid State Electrochem.* **21** (2017) 2707 (<http://dx.doi.org/10.1007/s10008-017-3642-z>)
7. R. Animesh, A. Sudhir, W. Yogesh, S. Manish, U. Govind, R. Sunit, P. Kashinath, G. Suresh, C. Ratna, *J. Solid State Electrochem.* **21** (2016) 9 (<http://dx.doi.org/10.1007/s10008-016-3328-y>)
8. B. Ruiz-Camacho, A. Medina-Ramírez, R. Fuentes-Ramírez, C. M. Gómez, *J. Solid State Electrochem.* **21** (2017) 2449 (<http://dx.doi.org/10.1007/s10008-017-3567-6>)
9. A. N. Correia, M.X. Façanha, P. Lima-Neto, *Surf. Coat. Technol.* **201** (2007) 7216 (<http://dx.doi.org/10.1016/j.surfcoat.2007.01.029>)
10. I. A. Carlos, E. D. Bidoia, E. M. J. A. Pallone, M. R. H. Almeida, C. A. C. Souza, *Surf. Coat. Technol.* **157** (2002) 14 (PII:S0257-8972(02)00139-1)
11. E. Rudnik, *Ionics* **19** (2013) 1047 (<http://dx.doi.org/10.1007/s11581-012-0819-4>)
12. M. Biçer, İ. Şışman, *Appl. Surf. Sci.* **257** (2012) 2944 (<http://dx.doi.org/10.1016/j.apsusc.2010.10.096>)
13. B. Tutunari, I. Prunaru, *An. Univer. Bucuresti Chim.* **18** (2009) 67
14. F. Xiao, X. Shen, F. Ren, A. A. Volinsky, *Int. J. Minerals Metall. Mater.* **20** (2013) 472 (<http://dx.doi.org/d10.1007/s12613-013-0753-0>)
15. A. Sharma, K. Dasa, H. J. Fecht, S. Das, *Appl. Surf. Sci.* **314** (2014) 516 (<http://dx.doi.org/10.1016/j.apsusc.2014.07.037>)
16. F. J. Barry, V. J. Cunnane, *J. Electroanal. Chem.* **537** (2002) 151 ([https://doi.org/10.1016/S0022-0728\(02\)01266-4](https://doi.org/10.1016/S0022-0728(02)01266-4))
17. C. T. J. Low, F. C. Walsh, *Electrochim. Acta* **53** (2008) 5280 (<http://dx.doi.org/10.1016/j.electacta.2008.01.093>)
18. A. Collazo, R. Figueroa, X. R. Nόvoa, C. Pérez, *Surf. Coat. Technol.* **280** (2015) 8 (<http://dx.doi.org/10.1016/j.surfcoat.2015.08.052>)
19. E. Gómez, E. Guauas, F. Sanz, E. Vallés, *J. Appl. Electrochem.* **465** (1999) 63 (<https://doi.org/10.1023/A:1024439023251>)
20. C. Han, Q. Liu, D. G. Ivey, *Electrochim. Acta* **54** (2009) 3419 (<http://dx.doi.org/10.1016/j.electacta.2008.12.064>)
21. Y. Goh, A. S. M. A. Hasseb, M. F. M. Sabri, *Electrochim. Acta* **90** (2013) 265 (<http://dx.doi.org/doi:10.1016/j.electacta.2012.12.036>)
22. B. Tutunari, A. Samide, *Optoelect. Adv. Mater.* **2** (2008) 659
23. J. L. P. Siqueira, I. A. Carlos, *J. Power Sources* **177** (2008) 211 (<http://dx.doi.org/10.1016/j.jpowsour.2007.11.02>)
24. X. Huang, Y. Chen, J. Zhou, Z. Zhang, J. Zhang, *J. Electroanal. Chem.* **709** (2013) 83 (<http://dx.doi.org/10.1016/j.jelechem.2013.09.012>)

25. B. Neveu, F. Lallemand, G. Poupon, Z. Mekhalif, *Appl. Surf. Sci.* **252** (2006) 3561 (<http://dx.doi.org/10.1016/j.apsusc.2005.05.024>)
26. N. M. Martyak, R. Seefeldt, *Electrochim. Acta* **49** (2004) 4303 (<http://dx.doi.org/10.1016/j.electacta.2004.03.039>)
27. H. Wang, M Pritzker, *Electrochim. Acta* **53** (2008) 2430 (<http://dx.doi.org/10.1016/j.electacta.2007.10.023>)
28. S. Joseph, G. J. Phatak, *Mater. Sci. Eng., B* **168** (2010) 219 (<http://dx.doi.org/10.1016/j.mseb.2010.01.017>)
29. C. Han, Q. Liu, D. G. Ivey, *Electrochim. Acta* **53** (2008) 8332 (<http://dx.doi.org/10.1016/j.electacta.2008.06.037>)
30. C. T. J. Low, F. C. Walsh, *Surf. Coat. Technol.* **202** (2008) 1339 (<http://dx.doi.org/10.1016/j.surfcoat.2007.06.032>)
31. M. R. Lee, S. H. Na, H. S. Park, S. J. Suh, *J. Nanosci. Nanotechnol.* **14** (2014) 9560 (<http://dx.doi.org/10.1166/jnn.2014.1017>)
32. U. Sahaym, S. L. Miller, M. G. Norton, *Mater. Lett.* **64** (2010) 1547 (<http://dx.doi.org/10.1016/j.matlet.2010.04.036>)
33. H. M. Maltanova, T. N. Vorobyova, O. N. Vrublevskaya, *Surf. Coat. Technol.* **254** (2014) 388 (<http://dx.doi.org/10.1016/j.surfcoat.2014.06.04>)
34. H. Hosoya, J. Tanaka and S. Nagakura, *Bull. Chem. Soc. Japan* **33** (1960) 850 (<http://doi.org/10.1246/bcsj.33.850>)
35. G. Cui, X. Ke, H. Liu, J. Zhao, S. Song, P. K. Shen, *J. Phys. Chem., C* **112** (2008) 13546 ([http://dx.doi.org/10.1021/jp8018099 CCC: \\$40.75](http://dx.doi.org/10.1021/jp8018099))
36. B. Scharifker, G. Hills, *Electrochim. Acta* **28** (1983) 879 ([http://doi.org/10.1016/0013-4686\(83\)85163-9](http://doi.org/10.1016/0013-4686(83)85163-9))
37. M. Palomar-Pardavé, B. Scharifker, E. M. Arce, M. Romero-Romo, *Electrochim. Acta* **50** (2005) 4736 (<http://dx.doi.org/10.1016/j.electacta.2005.03.004>)
38. J. Lei, J.G. Yang, *J. Chem. Technol. Biotechnol.* **92** (2017) 891 (<http://dx.doi.org/10.1002/jctb.5070>)
39. L. A. Azpeitia, C. A. Gervasi, A. E. Bolz'an, *Electrochim. Acta* **257** (2017) 388 (<http://doi.org/doi:10.1016/j.electacta.2017.10.064>).